



#### **OPEN ACCESS**

EDITED BY Xihui Shen, Northwest A&F University, China

REVIEWED BY Peibo Yuan. Southern Medical University, China Ricardo Mazzon. Federal University of Santa Catarina, Brazil

\*CORRESPONDENCE Yifana Cui Fuzhou Xu 

RECEIVED 20 July 2025 ACCEPTED 08 September 2025 PUBLISHED 25 September 2025

#### CITATION

Cui Y, Chen J, Feng X, Guo F, Shao Y and Xu F (2025) Transcriptomic and proteomic profiling of Actinobacillus pleuropneumoniae responses to iron starvation. Front, Cell, Infect, Microbiol, 15:1669654. doi: 10.3389/fcimb.2025.1669654

#### COPYRIGHT

© 2025 Cui, Chen, Feng, Guo, Shao and Xu. This is an open-access article distributed under the terms of the Creative Commons Attribution License (CC BY). The use, distribution or reproduction in other forums is permitted, provided the original author(s) and the copyright owner(s) are credited and that the original publication in this journal is cited, in accordance with accepted academic practice. No use, distribution or reproduction is permitted which does not comply with these terms.

# Transcriptomic and proteomic profiling of Actinobacillus pleuropneumoniae responses to iron starvation

Yifang Cui<sup>1\*</sup>, Jiahe Chen<sup>1,2</sup>, Xu Feng<sup>1,3</sup>, Fangfang Guo<sup>1</sup>, Yuxin Shao<sup>1</sup> and Fuzhou Xu<sup>1\*</sup>

<sup>1</sup>Beijing Key Laboratory for Prevention and Control of Infectious Diseases in Livestock and Poultry, Institute of Animal Husbandry and Veterinary Medicine, Beijing Academy of Agricultural and Forestry Sciences, Beijing, China, <sup>2</sup>College of Animal Science and Technology, Beijing University of Agriculture, Beijing, China, <sup>3</sup>College of Agriculture and Animal Husbandry, Qinghai University, Xining, China

Background: Actinobacillus pleuropneumoniae (APP) is the causative agent of porcine contagious pleuropneumonia, which remains a major pathogen endangering the swine industry. However, the mechanisms underlying its colonization and pathogenesis in pigs remain largely unknown.

Methods: An integrated analysis combining transcriptomic and proteomic profiling was employed to detect genetic and protein changes in APP under iron starvation.

Results: In total, 458 differentially expressed genes (DEGs) from the transcriptome and 532 differentially expressed proteins (DEPs) from the proteome were identified. The comparative analysis showed that 137 differentially expressed genes/proteins were shared between DEGs and DEPs, with the majority exhibiting consistent regulatory changes at both transcription and protein levels. Functional enrichment analysis revealed that the downregulated genes were predominantly associated with the generation of precursor metabolites and energy (45/105, 42.86%), primary metabolic process (29/105, 27.62%), ion binding (20/105, 19.05%), and metal cluster binding (18/105, 17.14%), corresponding to pathways involved in primary metabolites and energy biosynthesis and cellular respiration. Conversely, the upregulated genes were primarily enriched in iron transport (11/30, 36.67%) and iron binding (9/30, 30%), which corresponded to the iron starvation conditions. The expression changes of iron utilization systems, including TonB-ExbB-ExbD and some TonB-dependent receptors, by qRT-PCR were consistent with the results in both transcriptome and proteome analyses.

Conclusion: This study provided a global perspective on the response mechanisms employed by APP to iron starvation, characterized by suppressing electron transport and energy metabolism pathways and upregulating the pathways associated with the TonB-ExbB-ExbD energy transduction system for iron acquisition.

Actinobacillus pleuropneumoniae, transcriptome, proteome, iron starvation, virulence factor, adaptation

### 1 Introduction

Actinobacillus pleuropneumoniae (APP) is the causative agent of porcine infectious pleuropneumonia (PCP), a highly contagious respiratory disease affecting swine (Sassu et al., 2018). Infection with APP not only causes acute high mortality in pigs but also persists in the tonsils and lungs of subclinical infected pigs, triggering potential epidemic outbreaks (de Almeida et al., 2025). APP is classified into 2 biotypes and 19 serovars (Stringer et al., 2021). However, the cross-immune protection among different serovars is weak, which poses great challenges for controlling PCP (Sassu et al., 2018). Current commercial vaccines and control measures offer limited protection against APP infection. Therefore, it is necessary to develop novel and efficient prevention and control strategies.

Iron is an essential element for bacteria, participating in diverse cellular processes including respiration, ATP generation, and DNA replication and repair (Cassat and Skaar, 2013; Kramer et al., 2020). Additionally, the iron acquisition of pathogenic bacteria modulates their pathogenicity (Spiga et al., 2023). The host employs nutritional immunity, sequestering free iron through iron-binding proteins (such as transferrin and lactoferrin), compelling APP to utilize efficient iron acquisition systems to maintain survival and pathogenicity (Frost and Drakesmith, 2025). Therefore, the iron acquisition system is generally recognized as a major virulence factor in pathogenic bacteria (Buettner et al., 2009). Several iron transport systems have been identified in APP, including a transferrin receptor complex (TbpA/TbpB), a hydroxamate siderophore receptor (FhuA), and a hemoglobin-binding receptor (HgbA) (Jacques, 2004). It has also been shown that APP can use exogenous siderophores and may secrete endogenous chelators in response to iron starvation (Jacques, 2004). Studies have shown that TbpB exhibits serovar specificity (serovars 1, 5, and 7 of APP), and antibodies against TbpB can block iron uptake in these serovars (del Río et al., 2005). Consequently, the iron transporters of APP represent promising targets for vaccine design.

Bacteria possess adaptive mechanisms to cope with changing environments, including nutrient limitations and various stresses. This adaptation involves extensive reprogramming of gene expression and the specific induction or repression of key genes (Moreno-Gámez, 2022). Omics is often used to explore the expression patterns of global genes in bacteria. Transcriptional profiling of APP under iron-restricted conditions has been reported (Nielsen and Boye, 2005; Deslandes et al., 2007; Klitgaard et al., 2010). However, single-transcriptome analysis fails to capture all possible post-transcriptional regulatory mechanisms and translational regulation. The combination of transcriptome and proteome can reveal the mechanisms across complementary molecular levels. In this study, we performed an integrated analysis of transcriptomic and proteomic data to comprehensively investigate the mechanisms employed by APP in response to iron starvation. These findings establish a foundation for further deciphering the colonization and pathogenic mechanisms of APP in pigs and provide new insights for the development of control strategies.

### 2 Materials and methods

### 2.1 Strain and growth conditions

Actinobacillus pleuropneumoniae serovar 1 reference strain 4074 (ATCC 27088) was routinely cultured in tryptic soy broth (TSB, Difco, Sparks, MD, USA) or on agar supplemented with 5  $\mu$ g/mL of nicotinamide adenine dinucleotide (NAD, Merck KGaA, Darmstadt, Germany) at 37°C. According to the results of the pilot studies (Supplementary Figure S1), 20  $\mu$ M of deferoxamine mesylate (DFO, Merck KGaA, Darmstadt, Germany) was added to the TSB medium to establish an iron-restricted condition, and the TSB medium without supplements was used as the control.

### 2.2 RNA sample preparation

To determine the expression of genes related to iron utilization in APP, the experiment was divided into two groups: APP cultured in TSB + NAD medium serving as the control group and APP cultured in TSB + NAD + DFO medium under iron-restricted conditions serving as the iron-restricted group. The specific operations are as follows: fresh cultivated APP cells were harvested to collect the bacterial cells. Cell pellets were resuspended and washed with sterile PBS. APP in the control group was resuspended in TSB + NAD medium (group control), and the iron-restricted group was resuspended in TSB + NAD + DFO medium (group DFO). Bacterial suspensions were adjusted to approximately 10<sup>5</sup> CFU/mL. Cultures were incubated at 37°C with shaking at 200 rpm for 4 h. Finally, APP cells from each group were collected by centrifugation for RNA extraction. The total RNA was extracted using TRIzol<sup>TM</sup> reagent (Thermo Fisher Scientific Inc., USA) according to the manufacturer's instructions. Only a highquality RNA sample (RNA quality number ≥ 8.0) was used to construct the sequencing library.

# 2.3 Transcriptome sequencing and data processing

The collected RNA samples were subjected to RNA-seq transcriptome sequencing (Shanghai Majorbio Bio-pharm Technology Co., Ltd., Shanghai, China). The RNA-seq library was prepared using the Illumina Stranded mRNA Prep Ligation method and sequenced on the NovaSeq X Plus platform (PE150). High-quality clean reads were obtained and aligned to the reference genome (APP serovar 1 strain 4074, GenBank accession number CP029003.1) for sequence mapping and alignment analysis. Gene expression levels were quantified using the transcripts per million (TPM) reads method. The RSEM software (http://deweylab.github.io/RSEM/) was used to quantify gene abundance. Differential gene expression analysis was performed using the DESeq2 software (http://bioconductor.org/packages/stats/bioc/DESeq2/). Genes exhibiting a log2 fold change (log2FC) ≥1 and

an adjusted P-value (FDR) <0.05 were considered to be differentially expressed genes (DEGs). In addition, the identified DEGs were subjected to the Gene Ontology database for functional annotation and enrichment analysis.

### 2.4 Protein sample preparation

Proteomic sample preparation followed transcriptomic protocols (Section 2.2). Total proteins from the control and DFO groups were dissolved in a protein lysate solution containing 8 M of urea, 1% SDS, and a protease inhibitor cocktail. After lysis, proteins were digested with trypsin. The resulting peptide fragments were reconstituted in 0.1% trifluoroacetic acid, desalted using an Oasis HLB column (Waters Corporation, Framingham, MA, USA), and quantified by NanoDrop TM One (Thermo Fisher Scientific Inc., USA) prior to mass spectrometry detection.

# 2.5 Proteome sequencing and data processing

The peptide samples from different treatment groups were analyzed by a Vanquish Neo system coupled with an Orbitrap Astral mass spectrometer (Thermo Fisher Scientific Inc., USA) via the Majorbio platform. The chromatography run time was set to 8 min. Data-independent acquisition (DIA) was performed using an Orbitrap Astral mass spectrometer operated in DIA mode. The mass spectrometry scanning range was 100–1,700 *m/z*. DIA raw data were processed and searched using the Spectronaut software (Biognosys Inc., Newton, MA, USA). Protein quantification was performed using the MaxLFQ algorithm.

The database used for proteomic data analysis was the proteome of *Actinobacillus pleuropneumoniae* in the UniProt database (https://www.uniprot.org/), supplemented with annotation results derived from our transcriptome sequencing. Analogous to the transcriptomic analysis, the proteomics data were analyzed by calculating the relative protein expression ratio between groups and the corresponding *P*-value from statistical tests. Fold change and *P*-values for the proteins between the two groups were calculated using the "*t*-test" function in R. Proteins meeting the thresholds of fold change (FC) >1.2 or FC <0.83 and *P*-value <0.05 were defined as differentially expressed proteins (DEPs). Functional annotation and pathway enrichment analysis were performed on all identified proteins using the GO database and the KEGG database. Protein-protein interaction (PPI) networks were constructed using the STRING software (http://string-db.org).

# 2.6 Integrative analysis of transcriptome and proteome

An integrative analysis of transcriptomic and proteomic data was conducted to identify key factors and elucidate molecular mechanisms underlying iron utilization in APP using the Majorbio Cloud platform (https://cloud.majorbio.com/) (Han et al., 2024). The DEG and DEP sets were cross-referenced to identify shared genes/ proteins. A union set of all DEGs and DEPs was also generated. Genes related to iron utilization within the intersection and union sets were identified, and the correlation between mRNA and protein expression levels for these selected genes was assessed.

# 2.7 Validation of DEGs by quantitative reverse transcription PCR

The expression of selected upregulated DEGs associated with iron acquisition was validated by quantitative reverse transcription PCR (qRT-PCR). RNA samples, prepared identically to those used for transcriptome and proteome sequencing, were utilized for validation. The selected genes and primer information are listed in Supplementary Table S1. 16S rRNA served as the endogenous control (Li et al., 2024). The qRT-PCR assay was performed using the CFX96 Connect TM Real-Time PCR System (Bio-Rad Laboratories, Hercules, CA, USA). The thermal cycling parameters were initial denaturation at 95°C for 3 min, followed by 39 cycles of denaturation at 95°C for 10 s, and annealing at 60°C for 30 s. A melting curve analysis from 60°C to 95°C was conducted after the amplification reaction. Relative gene expression was calculated using the 2-ΔΔCt method (Livak and Schmittgen, 2001).

### 2.8 Statistical analysis

Statistical analyses were performed using Student's t-test and one-way ANOVA by GraphPad Prism 8 (San Diego, CA, USA). Data were presented as means  $\pm$  standard deviations. A P-value <0.05 was considered statistically significant.

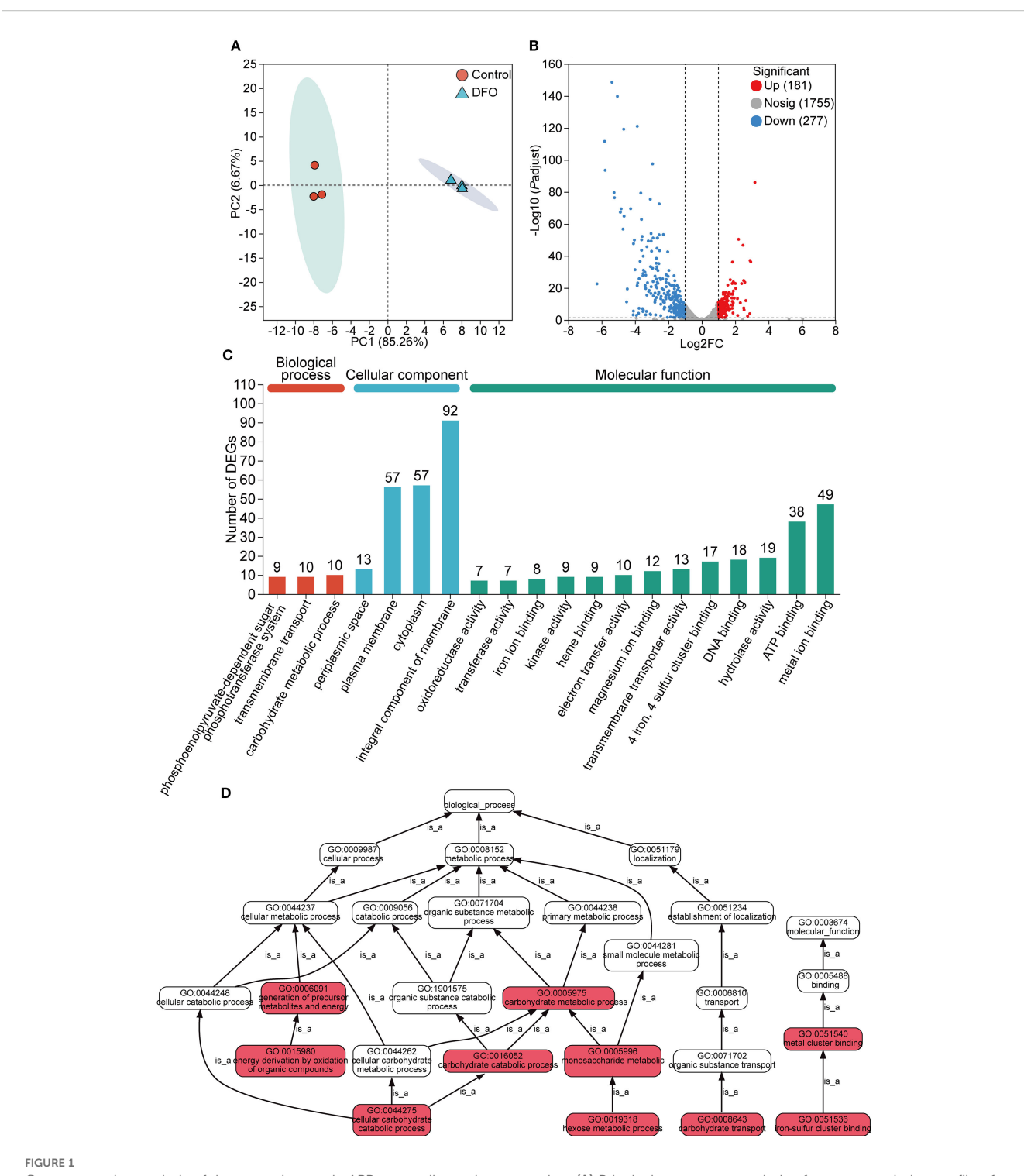
### 3 Results and discussion

# 3.1 Identification and functional enrichment analysis of DEGs from the transcriptome

Firstly, principal component analysis (PCA) was performed to assess the overall distribution of the gene transcription profile. The iron-restricted and control groups with three independent biological replicates were clustered separately (Figure 1A), indicating high reproducibility within biological replicates and significant transcriptional differences between the two groups.

Gene expression levels between the iron-restricted and control samples were compared. A total of 458 DEGs were identified (Supplementary Table S2), comprising 437 annotated genes, 13 novel transcripts, and 8 small RNAs (sRNAs). Among these DEGs, 181 were significantly upregulated and 277 were significantly downregulated in response to iron starvation (Figure 1B).

All the DEGs underwent GO term annotation and enrichment analysis. The DEGs were annotated into three GO categories, including biological process (BP), cellular component (CC), and



Gene expression analysis of the transcriptome in APP responding to iron starvation. (A) Principal component analysis of gene transcription profile of APP under iron-restricted conditions compared with the control group. (B) Differentially expressed genes (DEGs) with upregulation and downregulation between the iron-restricted and control groups. (C) Functional annotation of DEGs based on the GO database. The number of DEGs was labeled on the top of bars. (D) GO pathway enrichment analysis of DEGs. Red boxes indicated that DEGs were significantly enriched in the GO term. Each "is\_a" link along the arrow direction represented the subclass relationship.

molecular function (MF), with significant enrichment observed for 29 terms in BP, 219 in CC, and 216 in MF (Figure 1C). Within the MF category, terms related to metal ion binding and transfer were significantly enriched. The top significantly enriched GO pathways

for all 458 DEGs are shown in Figure 1D. Key enriched pathways included cellular metabolic processes, encompassing subcategories such as the establishment of localization and transport of cellular carbohydrate and organic substances.

# 3.2 Identification and functional enrichment analysis of DEPs from the proteome

PCA analysis of the proteomic data also revealed substantial changes in the protein profile of APP under iron starvation compared to the control (Figure 2A). A total of 532 DEPs were identified (Figure 2B, Supplementary Table S3), with 263 upregulated DEPs and 269 downregulated DEPs. Similar to the transcriptomic analysis, DEPs were annotated into the three main GO categories: BP, CC, and MF. Among these, 197 DEPs were enriched in ion binding, which was the most dominant subcategory (Figure 2C). The DEPs were significantly enriched in pathways involved in core cellular processes, particularly energy metabolism, respiration, and molecular interactions such as iron-sulfur cluster binding and electron transfer (Figure 2D).

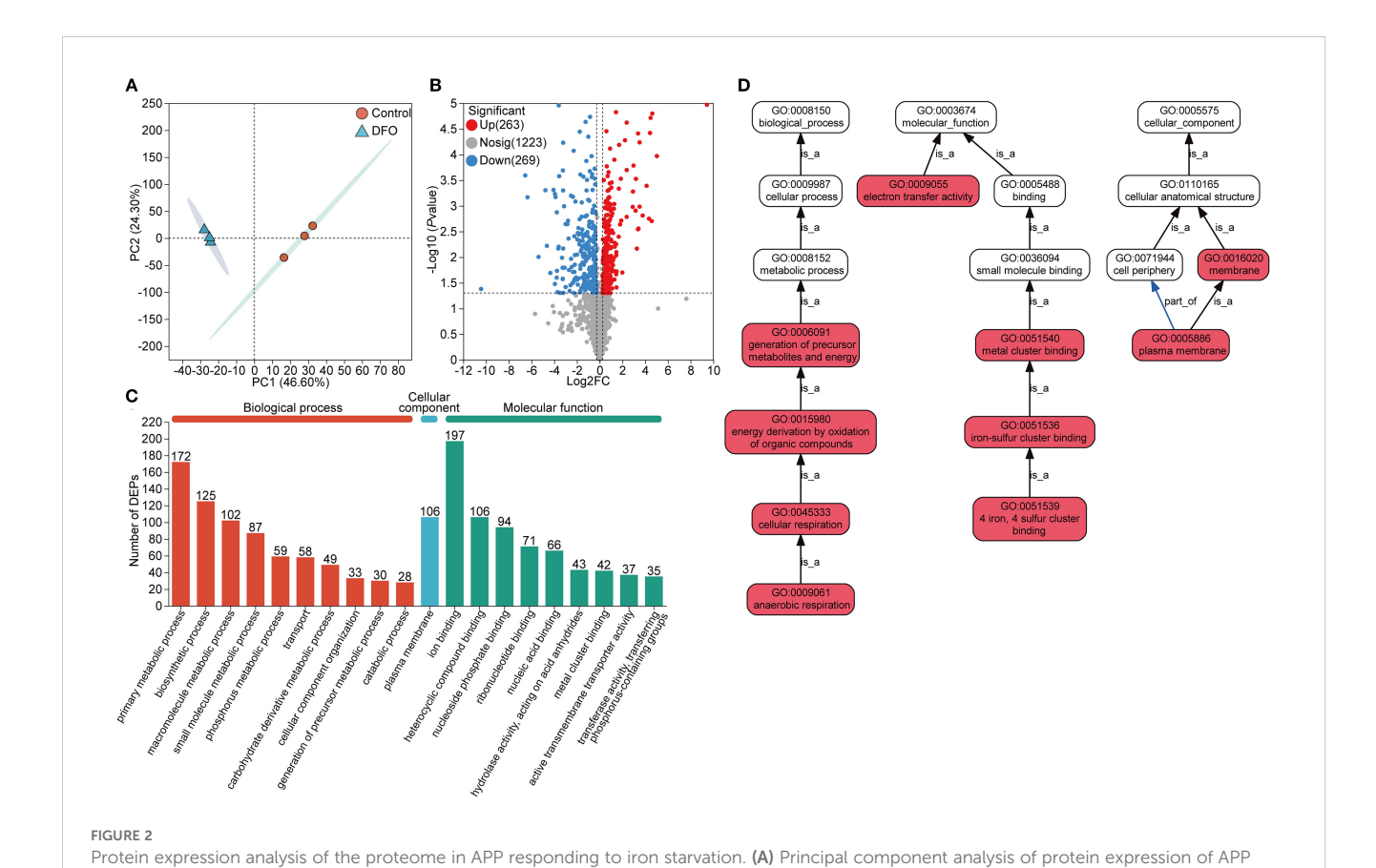
# 3.3 Integrated bioinformatic analysis of transcriptome and proteome

Integration of the 458 DEGs and 532 DEPs revealed that 137 genes and their corresponding proteins were shared between transcriptomic and proteomic analysis (Figure 3A). Among the 137 shared genes, 40

genes were significantly upregulated and 97 genes were significantly downregulated at the transcriptional level. Moreover, 32 proteins were significantly upregulated and 105 proteins were significantly downregulated referring to the proteome (Figure 3B). Furthermore, the up- or downregulated expression trends between the transcriptome and proteome were largely concordant for these genes. The fold change of upregulation was generally greater at the protein level compared to the transcriptional level. Discordant regulation between transcriptional and protein levels was observed for 28 genes (28/137, 20.44%, Supplementary Table S4).

The categories of the 137 genes were annotated through the GO database and enriched by the KEGG database (Figures 3C, D). Overall, the major annotated GO terms for the 137 shared genes included primary metabolic processes (34 genes), encompassing functions like generation of precursor metabolites and energy and oxidoreductase activity and ion binding (52 genes), including metal ion binding, metal cluster binding, and electron transfer. The expression levels of the shared 137 genes in APP under iron starvation in transcriptomic and proteomic sequencing are exhibited in Figure 3E.

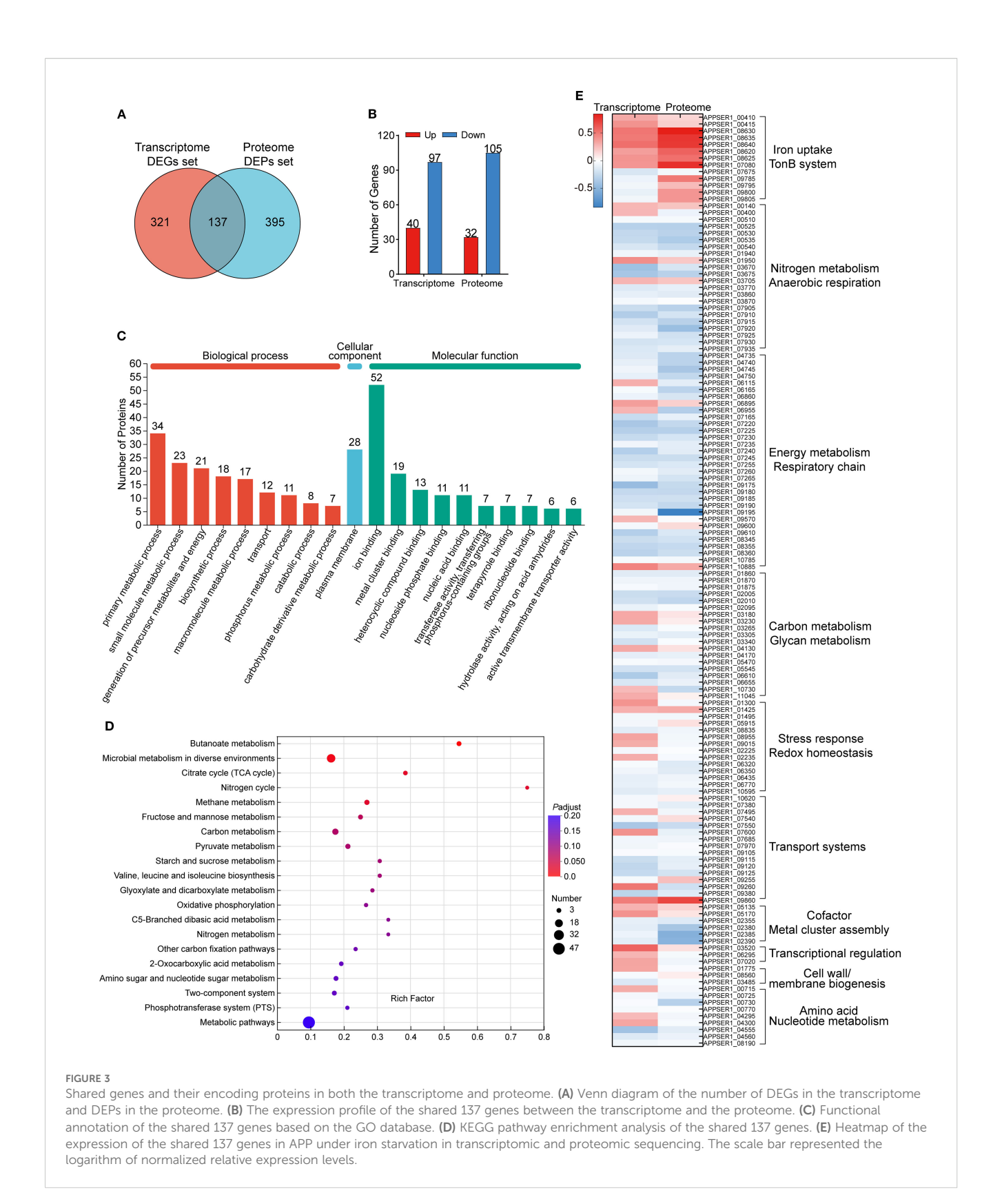
In addition, the enrichment of two datasets of genes/proteins in the metabolic pathways of APP was analyzed. One dataset consisted of the shared 137 DEPs/DEGs as described above, and the other dataset included 395 DEPs only detected in the proteome (with no



Frontiers in Cellular and Infection Microbiology

The "is\_a" denoted subclass relationships and the "part\_of" indicated inclusion relationships

under iron-restricted conditions compared with the control group. (B) Differentially expressed proteins (DEPs) with upregulation and downregulation between the iron-restricted and control groups. (C) Functional annotation of DEPs based on the GO database. The number of enriched proteins was labeled on the top of bars. (D) GO pathway enrichment analysis of DEPs. Red boxes indicated that DEPs were significantly enriched in the GO term.



significant differences at the transcriptional level). As shown in Supplementary Figure S2, the shared DEGs/DEPs were mainly enriched in pathways, including carbohydrate metabolism (amino sugar and nucleotide sugar metabolism), terpenoid and polyketide metabolism (terpenoid backbone biosynthesis), energy metabolism

(D-alanine metabolism, valine/leucine/isoleucine biosynthesis, TCA cycle), and the biosynthesis of other secondary metabolites (indole alkaloid biosynthesis, pantothenate and coenzyme A biosynthesis). Meanwhile, the DEPs only expressed at the protein level were mainly involved in lipid metabolism, carbohydrate

metabolism (lipopolysaccharide biosynthesis, interconversion between pentose and glucuronate), nucleotide metabolism (purine and pyrimidine metabolism), and the biosynthesis of other secondary metabolites (metabolism of arginine, proline, valine, leucine, and isoleucine).

# 3.4 Downregulated genes under iron starvation

The significantly downregulated DEGs (277/458, 60.48%) and DEPs (269/532, 50.56%) predominated in response to iron starvation, which revealed significant downregulation of irondependent pathways in APP, likely as an adaptation to conserve iron and mitigate an energy deficit. By cross-comparing the shared genes screened from transcriptomic and proteomic data, the proportions of downregulated genes were 70.80% (97/137) and 76.64% (105/137) in the transcriptome and proteome, respectively. Functional annotation and pathway enrichment analysis were performed on the 105 downregulated proteins identified in the proteome. The functional enrichment of these downregulated proteins is shown in Figure 4A. Within the BP category, the most enriched terms were "generation of precursor metabolites and energy" (45/105, 42.86%) and "primary metabolic process" (29/ 105, 27.62%). Within the MF category, "ion binding" (20/105, 19.05%) and "metal cluster binding" (18/105, 17.14%) were prominently enriched. Furthermore, pathway analysis revealed significant enrichment in primary metabolite and energy biosynthesis pathways, as well as cellular respiration (Table 1). The interaction network among these pathways is shown in Figure 4B. In agreement with previous reports (Deslandes et al., 2007; Klitgaard et al., 2010), APP primarily suppresses electron transport and energy metabolism pathways under iron starvation.

### 3.4.1 Anaerobic respiratory chains

The anaerobic respiratory chains were coordinately downregulated (Table 1). The dimethyl sulfoxide reductase (*dms* operon), fumarate reductase (*frd* operon), periplasmic nitrate reductase *nap* locus, the TMAO reductase (*tor* operon), and cytochrome C nitrite reductase (*nrf* operon) were significantly downregulated (Baez et al., 2022). APP likely downregulated iron-dependent anaerobic respiration to conserve iron (essential for Fe-S clusters and heme cofactors) and reduce reliance on this energy-generating pathway (Lill and Freibert, 2020). In addition, APP inhibited hydrogen metabolism. The genes involved in [Ni-Fe]-hydrogenase maturation (*hyp* operon) and hydrogenase structural subunits (*hya/hyb*) were strongly downregulated, potentially eliminating an alternative energy source in response to iron limitation (Rios-Delgado et al., 2025).

### 3.4.2 Energy metabolism pathways

The pathways involved in amino acid metabolism (*sda* and *lld*), glycogen metabolism (*glg*) and transport (*man*), and nitrogen metabolism (*nrf*) were downregulated, potentially reflecting their reliance on iron also. On the other side, APP prioritized core

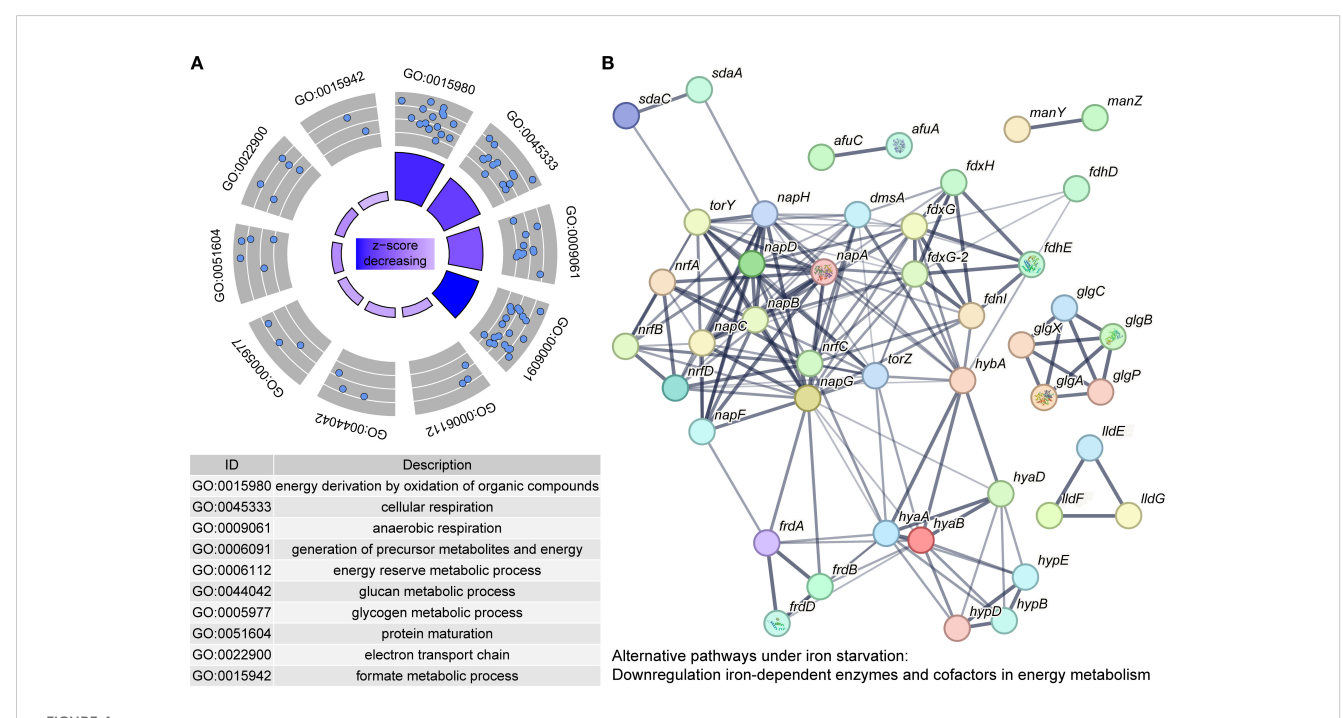


FIGURE 4
Downregulated genes in APP under iron starvation. (A) Enrichment of downregulated genes based on the GO database. Each blue dot represented a protein enriched in the GO term. The z-score in the inner circle was used to estimate the degree to which the pathway may be inhibited.

(B) A protein interaction network was constructed by protein-protein interaction information from the STRING database. Each node in the network represents a distinct protein, and the thickness of the edges connecting the nodes indicates the strength of evidence for the protein-protein interaction.

TABLE 1 Downregulated genes in the transcriptome and proteome of APP under iron starvation.

Gene		Accession	Transcriptom	ie	Proteome		
operon	Gene	ID <sup>a</sup>	Log2FC <sup>b</sup>	<i>P</i> -value	Log2FC	<i>P</i> -value	Description
	dmsA	APPSER1_09175	-6.27	1.03E-24	-3.09	1.60E-02	Dimethyl sulfoxide reductase subunit A
dms	dmsB	APPSER1_09180	-3.83	2.63E-25	-3.25	2.68E-02	Dimethylsulfoxide reductase subunit B
	dmsC	APPSER1_09185	-3.36	9.49E-22	-2.57	3.53E-02	Dimethyl sulfoxide reductase anchor subunit
	dmsD	APPSER1_09190	-2.90	5.17E-17	-3.25	2.63E-02	Tat proofreading chaperone DmsD
man	manZ	APPSER1_09115	-3.51	2.41E-31	-1.48	9.13E-03	PTS mannose transporter subunit IID
	manY	APPSER1_09120	-3.99	9.31E-34	-1.35	2.12E-02	PTS mannose/fructose/sorbose transporter subunit IIC
	manX	APPSER1_09125	-3.75	4.52E-28	-2.35	6.59E-04	PTS mannose transporter subunit IIAB
	frdD	APPSER1_08345	-3.49	1.97E-33	-2.46	1.55E-02	Fumarate reductase subunit D
	frdC	APPSER1_08350	-4.08	2.81E-50	_c	-	Fumarate reductase subunit FrdC
frd	frdB	APPSER1_08355	-4.03	1.47E-52	-3.13	1.01E-03	Succinate dehydrogenase/ fumarate reductase iron-sulfur subunit
	frdA	APPSER1_08360	-4.26	1.83E-72	-2.79	1.94E-03	Fumarate reductase (quinol) flavoprotein subunit
	napF	APPSER1_07905	-3.50	2.42E-42	-3.76	1.85E-02	Ferredoxin-type protein NapF
	napD	APPSER1_07910	-4.83	2.44E-72	-2.27	5.00E-02	Reductase
	napA	APPSER1_07915	-3.03	8.54E-57	-3.78	2.51E-02	Periplasmic nitrate reductase subunit alpha
nap	napG	APPSER1_07920	-2.37	9.29E-22	-5.38	9.89E-03	Ferredoxin-type protein NapG
	парН	APPSER1_07925	-1.63	1.56E-11	-2.52	1.08E-02	Quinol dehydrogenase ferredoxin subunit NapH
	парВ	APPSER1_07930	-2.94	1.21E-34	-2.22	1.94E-02	Nitrate reductase
	парС	APPSER1_07935	-2.64	5.42E-54	-1.44	3.52E-02	Cytochrome C
	afuC	APPSER1_07675	-2.71	5.11E-41	-0.65	3.98E-02	Ferric ABC transporter ATP- binding protein
afu	afuB	APPSER1_07670	-	-	-	-	Iron ABC transporter permease
	afuA	APPSER1_07665	-3.18	6.79E-20	-0.89	2.02E-01	ABC transporters
	hypВ	APPSER1_07220	-5.22	1.75E-79	-3.24	1.95E-04	Hydrogenase nickel incorporation protein HypB
	hypD	APPSER1_07225	-4.65	1.03E-67	-3.94	5.76E-04	Hydrogenase formation protein HypD
hyp	hypE	APPSER1_07230	-3.69	4.52E-39	-2.23	3.91E-03	Hydrogenase expression/ formation protein HypE
	hypF	APPSER1_07235	-1.48	1.23E-23	-1.53	6.16E-03	Carbamoyltransferase HypF
	hyaA	APPSER1_07240	-4.71	1.42E-59	-1.61	3.99E-02	Hydrogenase 2 small subunit

TABLE 1 Continued

Gene		Accession	Transcriptome		Proteome		5	
operon	Gene	ID <sup>a</sup>	Log2FC <sup>b</sup>	<i>P</i> -value	Log2FC	<i>P</i> -value	Description	
	hybA	APPSER1_07245	-3.60	1.01E-52	-2.84	2.27E-03	Hydrogenase 2 operon protein HybA	
		APPSER1_07250	-2.57	1.27E-37			Ni/Fe-hydrogenase cytochrome b subunit	
	hyaB	APPSER1_07255	-2.91	6.94E-54	-1.93	3.39E-03	Hydrogenase 2 large subunit	
	hyaD	APPSER1_07260	-1.31	5.71E-09	-1.58	8.51E-04	HyaD/HybD family hydrogenase maturation endopeptidase	
	hybE	APPSER1_07265	-1.60	4.41E-16	-2.29	7.46E-05	Hydrogenase-2 assembly chaperone	
	fdhD	APPSER1_04730	-0.22	2.65E-01			Formate dehydrogenase accessory sulfur transferase FdhD	
	fdoG	APPSER1_04735	-2.45	1.86E-27	-3.64	6.79E-03	Sulfate ABC transporter substrate-binding protein	
fdo	fdnG	APPSER1_04740	-1.97	5.25E-25	-3.61	6.24E-03	Formate dehydrogenase-N subunit alpha	
	fdoH	APPSER1_04745	-1.56	2.22E-14	-4.65	6.01E-03	Formate dehydrogenase subunit beta	
	fdoI	APPSER1_04750	-1.90	3.85E-15	-3.31	1.03E-02	Formate dehydrogenase subunit gamma	
	fdhE	APPSER1_04755	-0.56	7.68E-04	-1.25	1.60E-03	Formate dehydrogenase accessory protein FdhE	
sda	sdaC	APPSER1_04555	-5.78	8.74E-97	-1.62	3.46E-03	Serine transporter	
Suu	sdaA	APPSER1_04560	-2.49	1.76E-28	-1.08	3.24E-03	L-serine ammonia-lyase	
tor	torZ	APPSER1_03670	-5.82	5.23E-115	-2.19	1.40E-02	Trimethylamine-N-oxide reductase TorA	
	torY	APPSER1_03675	-5.37	1.19E-152	-3.77	1.33E-03	Nitrate reductase	
	lldG	APPSER1_02380	-2.23	9.16E-13	-4.78	4.87E-04	Lactate utilization protein C	
lld	lldF	APPSER1_02385	-1.67	2.92E-07	-6.55	2.46E-04	Iron-sulfur cluster-binding protein	
	lldE	APPSER1_02390	-2.17	4.03E-16	-6.35	6.73E-04	(Fe-S)-binding protein	
	glgB	APPSER1_01855	-3.03	6.84E-23	-1.22	8.17E-02	1%2C4-alpha-glucan branching protein GlgB	
	glgX	APPSER1_01860	-2.27	6.86E-21	-1.69	4.70E-02	Glycogen debranching enzyme GlgX	
glg	glgC	APPSER1_01865	-2.70	3.59E-34	-1.70	8.87E-02	Glucose-1-phosphate adenylyltransferase	
	glgA	APPSER1_01870	-1.56	2.01E-18	-0.96	3.89E-02	Glycogen synthase	
	glgP	APPSER1_01875	-1.12	1.45E-08	-0.90	8.02E-03	Glycogen/starch/alpha-glucan phosphorylase	
nrf	nrfA	APPSER1_00525	-4.50	4.13E-13	-3.94	3.32E-02	Ammonia-forming nitrite reductase cytochrome c552 subunit	
	nrfB	APPSER1_00530	-3.86	1.45E-23	-3.71	4.80E-02	Cytochrome c nitrite reductase pentaheme subunit	

TABLE 1 Continued

Gene	Gene	Accession ID <sup>a</sup>	Transcriptome		Proteome		Description
	operon		Log2FC <sup>b</sup>	P-value	Log2FC	<i>P</i> -value	Description
	nrfC	APPSER1_00535	-3.75	6.45E-09	-4.34	2.03E-02	Cytochrome c nitrite reductase Fe-S protein
	nrfD	APPSER1_00540	-2.76	9.20E-24	-3.19	4.97E-02	Cytochrome c nitrite reductase subunit NrfD

<sup>&</sup>lt;sup>a</sup>Accession ID in the genome of APP serovar 1 reference strain 4074 (CP029003.1).

metabolism and downregulated non-essential pathways, such as carbon source transport (*man* operon), catabolism (*fdo* operon and *lld* operon), glycogen synthesis (*glg* operon), amino acid utilization (*sda* operon), and the synthesis of iron-containing enzymes (such as Fe-S proteins) to promote survival under iron starvation (Klitgaard et al., 2010).

### 3.4.3 Classical iron-responsive elements

Due to the ferroxidase Dps of *Escherichia coli* that can protect bacteria from reactive oxygen species damage, the Dps-like protein FtpA in APP was also identified to possess a conserved ferritin domain containing a ferroxidase site, which plays critical roles in antioxidative stress and virulence (Tang et al., 2022). The *ftpA* gene (APPSER1\_08165) was downregulated under iron-restricted conditions at the transcript level. In addition, we also saw that multiple ribosomal proteins—L33, L34, L29, S20, L24, L31, L25, S5, S16, and L27—were downregulated (>2-fold) at the protein level under iron-restricted conditions. As the classical iron-responsive elements, the roles of ribosomal proteins in iron homeostasis of APP need to be further investigated.

### 3.4.4 Other downregulated genes

Comparison of transcriptomic and proteomic profiles showed that the downregulated DEPs generally followed the same trend as the downregulated DEGs. However, the magnitude of downregulation for proteins such as *afu* operon, *macA*, *ompW*, and *lamB* was less pronounced at the protein level than at the transcript level. Both *afuABC* and *macA* genes were regulated by *fur* and exhibited transcriptional upregulation under iron deficiency (Hsu et al., 2003). However, in this study, the transcription of *afuA*, *afuC*, and *macA* was significantly downregulated. This observation may reflect an adaptive strategy under extreme iron starvation by downregulating these genes to conserve ATP while switching to low-energy iron acquisition systems.

# 3.5 Upregulated genes under iron starvation

In addition to downregulating the bypass metabolic pathways, APP also actively enhanced iron transport to cope with iron starvation. We screened all DEGs (458) and DEPs (532) to identify significantly upregulated genes/proteins associated with

iron acquisition. Functional enrichment analysis of these upregulated entities revealed predominant association with iron transport (11/30, 36.67%) and iron binding (9/30, 30%) (Figure 5A). The expression profiles of key genes involved in iron acquisition, energy transduction, iron transport, transcriptional regulation, and stress resistance are detailed in Table 2. The interaction network among these pathways is shown in Figure 5B. The qRT-PCR results further confirmed the upregulation of *tonB-exbBD* systems and some specific TonB-dependent receptors, which were consistent with transcriptomic and proteomic analysis (Figure 6). The main upregulated gene clusters in APP upon iron-restricted conditions are listed below.

#### 3.5.1 TonB-ExbBD energy transduction systems

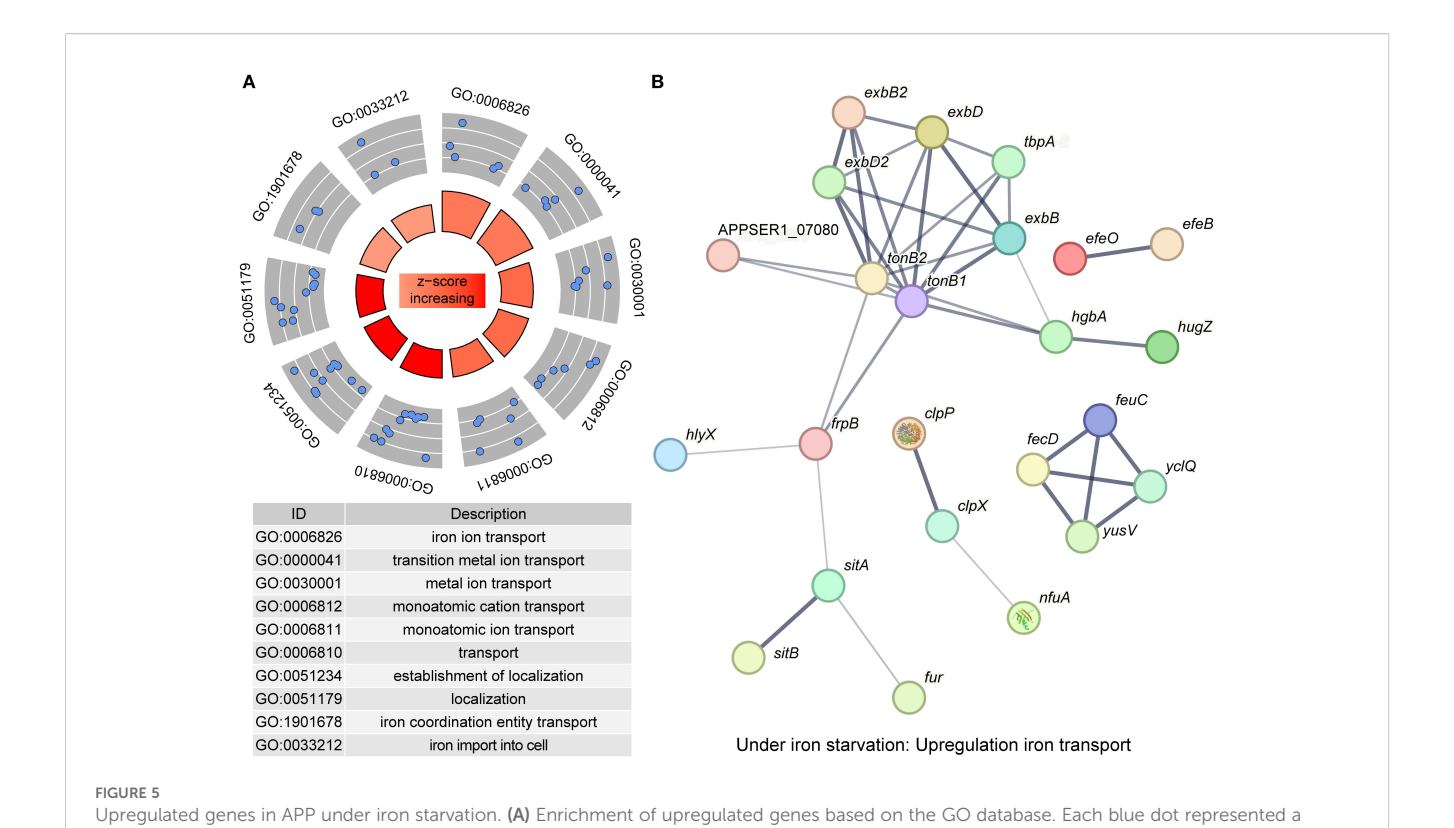
APP has two TonB-ExbBD systems, which play an essential role in iron homeostasis (Beddek et al., 2004). Previous studies showed that both systems were upregulated upon iron starvation, while the upregulation of *tonB2* was lower than in *tonB1* (Deslandes et al., 2007; Klitgaard et al., 2010). In this study, integrative transcriptomic and proteomic analysis revealed similar results (Table 2, Figure 6), and the TonB1-ExbB1-ExbD1 system exhibited significant upregulation with 6.25- and 21.59-fold increase of TonB1 at both the transcript and protein levels, respectively. In contrast, the TonB2-ExbB2-ExbD2 system showed moderate upregulation with 2.16- and 1.93-fold increase of TonB2, correspondingly. Collectively, these results confirm that APP significantly activated the TonB-ExbBD energy transduction systems under iron starvation.

#### 3.5.2 Iron uptake from host sources

APP can use host iron derived from hemoglobin or transferrin for growth in a process mediated by surface receptor proteins HgbA or TbpA/B, respectively (Baltes et al., 2002; Jacques, 2004; Srikumar et al., 2004). In addition to the similar transcriptomic upregulation (Deslandes et al., 2007; Klitgaard et al., 2010), proteomic analysis also showed that APP significantly upregulated transferrin receptors (11.42- and 9.13-fold for *tbpA* and *tbpB*) and the hemoglobin/heme system (13.75- and 11.41-fold for *hgbA* and *hutZ*) to compete for host iron sources (Table 2). Notably, an uncharacterized TonB-dependent receptor APPSER1\_07080, which was designated as a putative TonB-dependent haem receptor (APL\_1299; Klitgaard et al., 2010), exhibited dramatic upregulation with 3.40- and 24.77-fold at both the transcript and protein levels, respectively, potentially recognizing a novel or

<sup>&</sup>lt;sup>b</sup>Mean of three independent samples; FC, fold change.

<sup>&</sup>lt;sup>c</sup>No available data.



protein enriched in the GO term. The z-score in the inner circle was used to estimate the degree to which the pathway may be activated.

(B) A protein interaction network was constructed by protein-protein interaction information from the STRING database. Each node in the network represents a distinct protein, and the thickness of the edges connecting the nodes indicates the strength of evidence for the protein-protein

TABLE 2 Upregulated genes in the transcriptome and proteome of APP under iron starvation.

Formalian	Gene	Coro	Accession ID <sup>a</sup>	Transcript	tome	Proteome		5
Function	operon	Gene		Log2FC <sup>b</sup>	<i>P</i> -value	Log2FC	<i>P</i> -value	Description
		tonB1	APPSER1_08640	2.64	5.90E-14	4.43	2.80E-05	Energy transducer TonB
	tonB1-exbB1- exbD1	exbB1	APPSER1_08635	2.39	6.48E-25	4.48	9.33E-06	MotA/TolQ/ExbB proton channel family protein
TonB-exbBD		exbD1	APPSER1_08630	2.52	7.27E-27	5.03	9.72E-05	Biopolymer transporter ExbD
system	tonB2-exbB2- exbD2	tonB2	APPSER1_00405	1.11	5.26E-05	0.95	8.01E-02	Energy transducer TonB
		exbD2	APPSER1_00410	1.38	1.59E-05	0.94	2.98E-02	TonB system transport protein ExbD
		exbB2	APPSER1_00415	1.85	1.23E-15	1.06	1.91E-02	TonB-system energizer ExbB
Transferrin utilization system	tbp	tbpA	APPSER1_08620	1.58	1.60E-10	3.51	4.80E-05	Lactoferrin/ transferrin family TonB-dependent receptor
		tbpB	APPSER1_08625	1.80	1.22E-15	3.19	2.88E-04	

(Continued)

interaction.

TABLE 2 Continued

	Gene	C	Accession	Transcrip	tome	Proteome		Description
Function	operon	Gene	IDª	Log2FC <sup>b</sup>	<i>P</i> -value	Log2FC	<i>P</i> -value	Description
								Transferrin-binding protein-like solute binding protein
		fhuC	APPSER1_10940	0.60	1.84E-02	1.45	2.16E-02	Fe <sup>3+</sup> -hydroxamate ABC transporter ATP-binding protein FhuC
	fhu	fhuD	APPSER1_10945	0.80	1.31E-03	0.93	2.70E-02	Iron-siderophore ABC transporter substrate-binding protein
		fhuB	APPSER1_10950	0.25	2.46E-01	_c	-	Fe(3 +)-hydroxamate ABC transporter permease FhuB
Ferrichrome		fhuA	APPSER1_10955	-0.39	4.45E-02	-	-	TonB-dependent siderophore receptor
utilization system	fec	fecA	APPSER1_03805	0.36	3.55E-02	1.80	2.30E-03	Enterochelin ABC transporter substrate-binding protein
		fecB	APPSER1_03810	1.84	1.24E-38	1.24	1.00E-01	Iron ABC transporter permease
		fecC	APPSER1_03815	1.04	7.61E-07	1.06	6.93E-02	Iron ABC transporter permease
		fecD	APPSER1_03820	0.99	1.28E-06	1.17	1.43E-02	Iron ABC transporter ATP- binding protein
	cir	cirA	APPSER1_05110	0.21	2.66E-01	-0.33	1.30E-01	TonB-dependent receptor
Hemoglobin/ heme utilization	hgb	hgbA	APPSER1_05725	0.60	3.74E-03	3.78	1.54E-03	TonB-dependent hemoglobin/ transferrin/ lactoferrin family receptor
system		hutZ	APPSER1_05730	0.99	6.76E-07	3.51	1.03E-03	Heme utilization protein HutZ
T	fnr	hlyX/fnr	APPSER1_03520	2.90	1.25E-39	0.68	3.30E-02	Transcriptional regulator FNR
Transcription regulator	fur	fur	APPSER1_06640	0.75	1.52E-04	-	-	Ferric iron uptake transcriptional regulator
		copA	APPSER1_06865	-0.86	2.10E-06	1.47	8.01E-03	Cadmium- translocating P-type ATPase
Efflux pump systems	Acr	acrA	APPSER1_03195	-0.05	7.66E-01	0.70	2.55E-03	Efflux RND transporter periplasmic adaptor subunit
		acrB	APPSER1_03200	-0.12	3.99E-01	0.77	9.23E-04	Transporter

TABLE 2 Continued

	Gene	Carra	Accession	Transcript	tome	Proteome		Description
Function	operon	Gene	ID <sup>a</sup>	Log2FC <sup>b</sup>	<i>P</i> -value	Log2FC	<i>P</i> -value	Description
	sap	sapC	APPSER1_04235	0.30	5.76E-02	0.83	1.97E-03	Antimicrobial peptide ABC transporter permease SapC
		sapB	APPSER1_04240	0.26	1.19E-01	0.64	1.86E-01	Antimicrobial peptide ABC transporter permease SapB
		sapA	APPSER1_04245	-0.08	6.39E-01	0.46	6.43E-03	ABC transporter substrate-binding protein
		nfuA	APPSER1_00780	1.39	6.75E-11	0.47	1.49E-01	Iron-sulfur cluster biogenesis protein NfuA
		sitB	APPSER1_01425	1.13	9.76E-08	1.86	2.87E-04	Manganese transporter
Stress resistance	sit	sitA	APPSER1_01430	0.65	4.08E-04	3.16	1.23E-03	Metal ABC transporter substrate-binding protein
		efeO	APPSER1_03570	0.18	6.20E-01	3.27	6.81E-03	EfeM/EfeO family lipoprotein
	efe	efeB	APPSER1_03575	0.46	1.33E-02	3.42	2.76E-03	Deferrochelatase/ peroxidase EfeB
			APPSER1_03580	0.15	3.70E-01	3.37	2.85E-03	Fe <sup>2+</sup> /Pb <sup>2+</sup> permease
			APPSER1_01450	-0.01	9.63E-01	1.45	5.58E-03	TonB-dependent receptor
			APPSER1_07080	1.77	3.59E-11	4.63	5.90E-06	TonB-dependent receptor
		yclQ	APPSER1_03805	0.36	3.55E-02	1.80	2.30E-03	Enterochelin ABC transporter substrate-binding protein
Unknown		fecD	APPSER1_03810	1.84	1.24E-38	1.24	1.00E-01	Iron ABC transporter permease
		feuC	APPSER1_03815	1.04	7.61E-07	1.06	6.93E-02	Iron ABC transporter permease
		yusV	APPSER1_03820	0.99	1.28E-06	1.17	1.43E-02	Iron ABC transporter ATP- binding protein
		gntP	APPSER1_00740	-0.42	1.47E-01	4.58	1.97E-03	GntP family permease
		glxK	APPSER1_00745	-0.40	1.67E-01	4.34	1.77E-03	Glycerate kinase
		lldD	APPSER1_10140	0.76	2.97E-01	3.38	2.89E-05	Alpha-hydroxy-acid oxidizing enzyme
		chuW	APPSER1_08325	-0.18	4.91E-01	2.23	4.28E-05	Putative heme utilization radical SAM enzyme HutW

TABLE 2 Continued

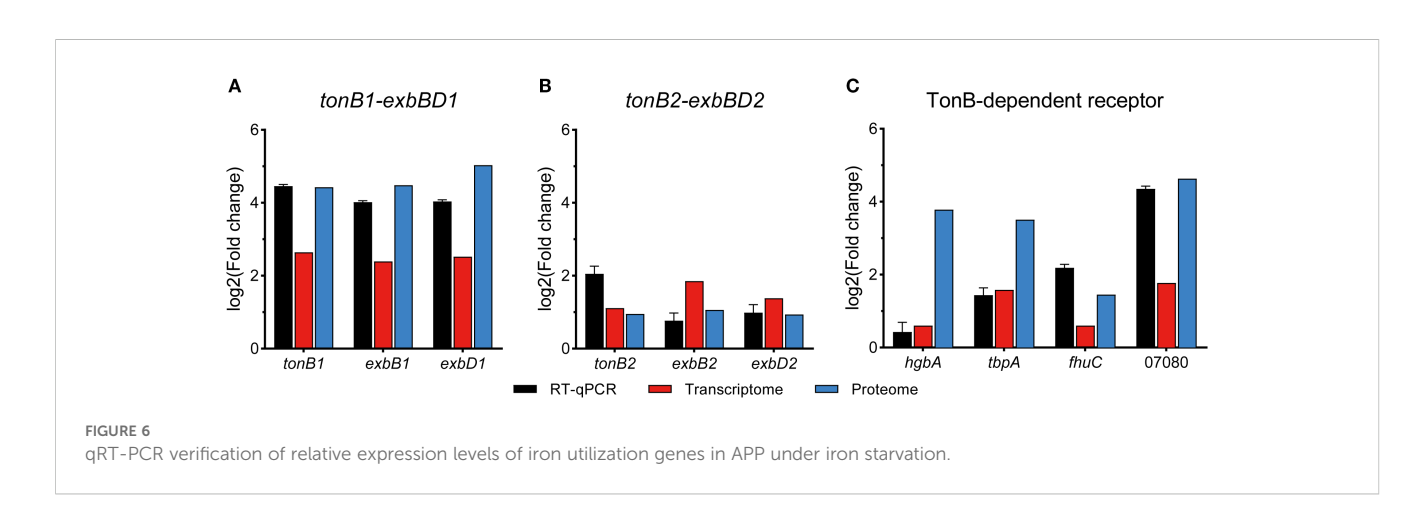
	Gene operon Gene	Como	Accession	Transcriptome		Proteome		Description
Function		Gene	ID <sup>a</sup>	Log2FC <sup>b</sup>	<i>P</i> -value	Log2FC	<i>P</i> -value	Description
			APPSER1_09785	-1.64	7.26E-06	2.98	1.54E-04	Iron ABC transporter substrate-binding protein
			APPSER1_09790	-0.88	3.75E-05	2.93	5.18E-04	Iron ABC transporter permease
			APPSER1_09795	-1.39	1.17E-08	1.49	1.90E-02	ABC transporter ATP-binding protein
			APPSER1_09800	-1.85	8.36E-15	2.38	1.63E-03	Pseudoazurin
			APPSER1_09805	-1.38	3.58E-13	2.38	1.91E-04	Iron ABC transporter substrate-binding protein
			APPSER1_09810	-0.14	4.94E-01	0.91	1.84E-03	Glutathione synthetase

<sup>&</sup>lt;sup>a</sup>Accession ID in the genome of APP serovar 1 reference strain 4074 (CP029003.1).

unknown iron transporter. The tellurite resistance gene *tehB*, which was predicted to be involved in haem utilization (Whitby et al., 2010; Klitgaard et al., 2010), was also upregulated 2.5-fold at the protein level. A putative *hpuB* gene cluster APPSER1\_10635 to APPSER1\_10645 involved in hemoglobin transport, corresponding to APL\_1953 to APL\_1955 in Klitgaard et al. (2010), had not been detected or showed no significant difference at both the transcript and protein levels, which was inconsistent with previous reports (Deslandes et al., 2007; Klitgaard et al., 2010). However, the adjacent genes APPSER1\_10650 and APPSER1\_10655 were upregulated at the transcript level, similar to previous reports (Deslandes et al., 2007; Klitgaard et al., 2010).

### 3.5.3 Iron uptake by siderophores

Siderophore-mediated iron acquisition plays an important role in bacterial growth and fitness under an iron-limited environment (Ellermann and Arthur, 2017). Currently, ferrichrome is the only identified ferric hydroxamate siderophore used by APP. The transcriptomic and proteomic analysis revealed no significant difference in the fhu operon except the modest increase of fhuC (2.74-fold at the protein level) and further confirmed that the ferrichrome receptor fhuA is not regulated by iron (Mikael et al., 2003; Deslandes et al., 2007; Klitgaard et al., 2010). Notably, APP was able to use exogenous catecholate siderophore such as enterobactin for growth (Diarra et al., 1996). It was predicted that the fec-like operon and the hypothetical cirA protein may encode the catecholate receptors (Klitgaard et al., 2010). The fec-like operon APPSER1\_03805 to APPSER1\_03820 was significantly upregulated at both transcript and protein levels, corresponding to the CeuBCDE system in Campylobacter enterobactin utilization (Miller et al., 2009). However, the cirA gene (APPSER1\_05110) showed no significant difference. The catecholatemediated iron uptake system in APP needs to be further investigated.



<sup>&</sup>lt;sup>b</sup>Mean of three independent samples; FC, fold change.

<sup>&</sup>lt;sup>c</sup>No available data.

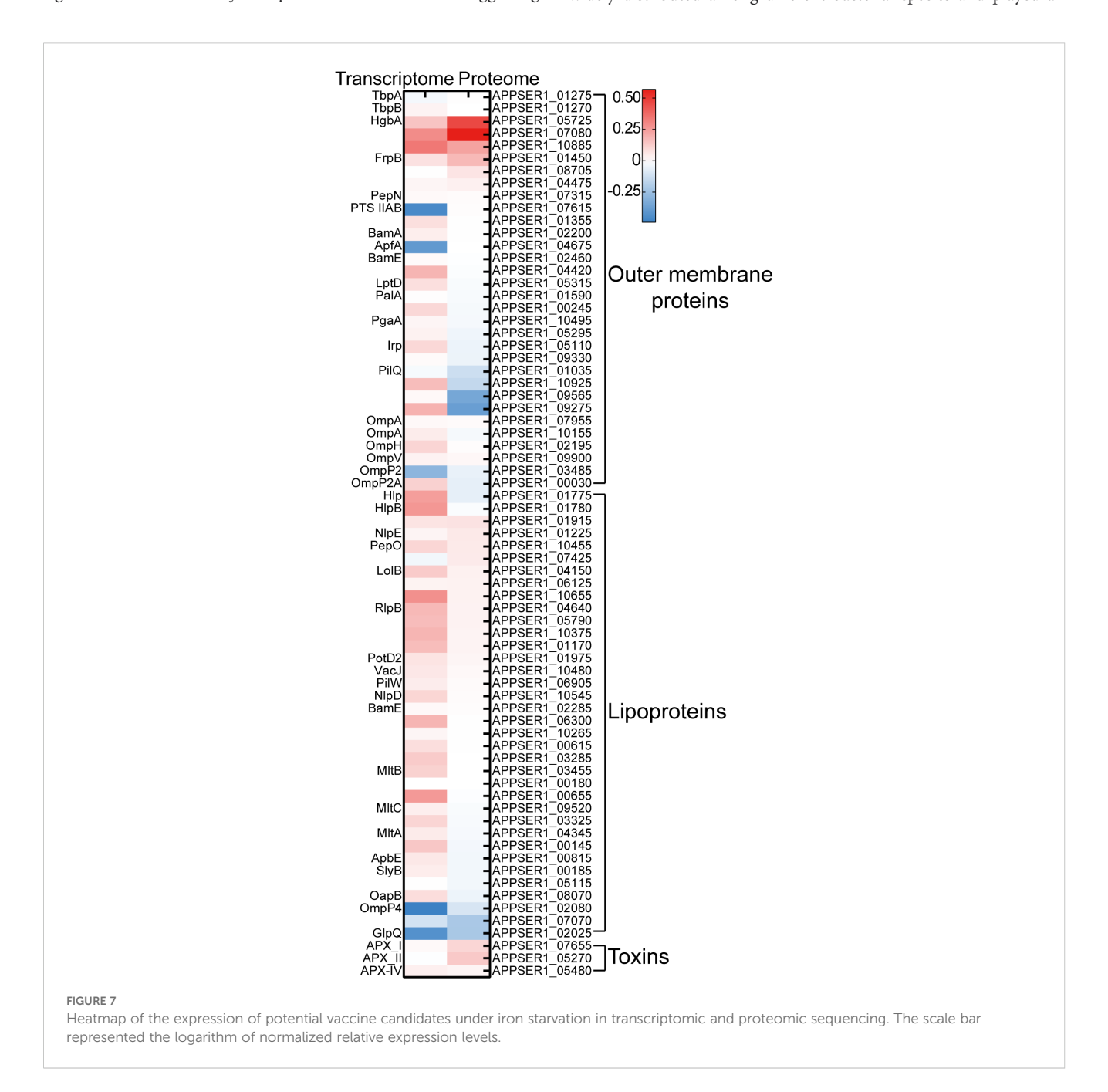
### 3.5.4 Transcriptional regulators

The iron-responsive transcriptional regulators HlyX (FNR) and Fur were involved in iron homeostasis in APP (Jacobsen et al., 2005; Buettner et al., 2009). The *hlyX* gene (APPSER1\_03520) was significantly upregulated at both the transcript and protein levels, likely coordinating the repression of iron-consuming processes (e.g., anaerobic metabolism) and potentially synergizing with other iron starvation responses (Buettner et al., 2009). Fur is recognized as a key positive regulator of APP virulence (Jacobsen et al., 2005), acting primarily as a repressor of virulence genes under iron-replete conditions, and this repression is alleviated during iron starvation (Stoffel and Drakesmith, 2024). In this study, no significant difference in *fur* expression was observed, suggesting

that iron deficiency may directly relieve *fur*-mediated repression without necessitating increased Fur protein abundance.

### 3.5.5 Efflux pump systems

To counteract the metal stress, bacteria have evolved a range of efflux pump systems, including the heavy metal efflux family, the P-type ATPase family, and the cation diffusion facilitator family (Sharma et al., 2023). The P-type ATPase CopA (APPSER1\_06865) in APP contributing to copper resistance was significantly upregulated at the protein level under iron-restricted conditions in this study (Peng et al., 2021; Klitgaard et al., 2010). Furthermore, the RND (resistance-nodulation-division) efflux pump AcrAB was widely distributed among different bacterial species and played an



essential role in antimicrobial resistance (Subhadra et al., 2020). The expression of *acrA/B* (APPSER1\_03195 and APPSER1\_03200) was significantly upregulated at the protein level in response to iron stress. Additionally, the Sap transporter system is important for resistance to antimicrobial peptides in some Gram-negative pathogens including APP (Xie et al., 2017). The Sap operon *sapABC* (APPSER1\_04235 to APPSER1\_04245) was also significantly upregulated at the protein level, which may be involved in iron transport.

### 3.5.6 Stress defense pathways

APP upregulated stress defense pathways to maintain metal homeostasis. The stress-resistant genes *nfuA* (Fe-S cluster assembly), *sit* (manganese transporter), and *efe* (low-pH Fe<sup>2+</sup> uptake/heme utilization) were all upregulated (Table 2). For instance, the Fe-S cluster assembly/repair pathway protein NfuA was induced, presumably to maintain the function of essential ironsulfur proteins (Lill and Freibert, 2020). The manganese uptake system (*sit* operon) was markedly upregulated, likely to combat iron starvation-induced oxidative stress (Dorman, 2023). The low-pH ferrous iron uptake and heme-derived iron utilization system (*efe* operon) was strongly elevated at the protein level, in agreement with previous reports (Deslandes et al., 2007; Klitgaard et al., 2010). The *efe* operon can enhance Fe<sup>2+</sup> import and heme-derived iron utilization, potentially contributing to peroxidase activity (Grosse et al., 2006).

#### 3.5.7 Other upregulated genes

We found that the GntP family permease APPSER1\_00740 and the glycerate kinase APPSER1\_00745 dramatically increased the expression at the protein level (23.9- and 20.2-fold, respectively), which were involved in gluconate uptake and gluconate phosphorylation (Qu et al., 2025). In agreement with previous reports (Deslandes et al., 2007; Klitgaard et al., 2010), the genes encoding L-lactate dehydrogenase LldD (APPSER1\_10140) and a putative heme utilization radical SAM enzyme ChuW (APPSER1\_08325) were both significantly upregulated at the protein level. An operon (APPSER1\_09785 to APPSER1\_09810), encoding putative iron transport-associated proteins, was also dramatically upregulated at the protein level. Notably, the gene encoding ribosome-bound ATPase RbbA (APPSER1\_04465) in E. coli, specifically bound to 70S ribosomes and 30S subunits (Kiel and Ganoza, 2001), showed the highest upregulation at the protein level (693.5-fold). These elevated expressions may represent a compensatory response of APP to accelerate iron acquisition, which also suggested to be the major virulence factors of APP (Soto Perezchica et al., 2023).

# 3.6 Exploring potential vaccine candidates in APP

Currently, commercially available vaccines of APP, including inactivated bacterins and subunit vaccines, have been licensed for use in pigs with clinical limitations such as side effects and low cross-protection (Zhang et al., 2022). Innovative vaccine development depends on exploring novel and effective antigen

candidates in bacteria (Loera-Muro and Angulo, 2018). Iron transporters and iron-regulated proteins, being major virulence factors, represent promising targets for vaccine development (Goethe et al., 2000; Stoffel and Drakesmith, 2024). For instance, the commercial subunit vaccines of APP include the iron-regulated proteins such as TbpA/B and OmlA (Loera-Muro and Angulo, 2018). Multiple iron transporters and iron-regulated proteins, including TbpA/B, OmlA, HgbA, LppC, and LolB, had been evaluated for the APP subunit vaccine (Loera-Muro and Angulo, 2018). The detergent extraction of APP cultures induced by iron restriction was also used for a subunit vaccine strategy (Goethe et al., 2000). The 2-D immunoblot-based proteomic and immunoproteomic analysis was used for exploring the potential APP subunit vaccines under iron-restricted conditions (Chung et al., 2012; Buettner et al., 2011). In this study, integrated transcriptomic and proteomic analysis revealed that iron starvation induced significant expression of a range of outer membrane proteins, lipoproteins, and Apx toxins (Figure 7); among them, several TonB-dependent receptors with undefined functions, such as APPSER1\_07080 and APPSER1\_10885, can be used for further investigation on subunit vaccine development.

### 4 Conclusion

This study aims to further analyze the adaptive mechanisms of APP under iron-restricted conditions. We seek to elucidate the mechanisms enabling APP to enhance growth and colonization within the host while maintaining iron homeostasis, utilizing transcriptomics to investigate regulatory responses and proteomics to validate functional protein expression. We observed significant changes at both the transcriptional and protein levels in the core metabolic cycles of APP. Simultaneously, under iron starvation conditions, APP activated multiple iron acquisition systems to enable efficient exploitation of host-associated iron, siderophores, and free Fe<sup>2+</sup>. In conclusion, integrative transcriptomic and proteomic profiling of APP under iron starvation provides a comprehensive understanding of the mechanisms underlying resource conservation and adaptation to iron stress in APP. Furthermore, the results highlight novel potential targets for developing vaccines against APP.

# Data availability statement

The datasets presented in this study can be found in online repositories. The raw data of transcriptomic sequencing are deposited in the NCBI database under the BioProject number PRJNA1284040. The proteomic data are deposited in the iProX database under the Project ID IPX0012451001.

### **Author contributions**

YC: Data curation, Formal Analysis, Funding acquisition, Project administration, Resources, Software, Visualization,

Writing – original draft, Writing – review & editing. JC: Data curation, Formal Analysis, Methodology, Software, Writing – original draft. XF: Formal Analysis, Methodology, Software, Writing – original draft. FG: Data curation, Writing – review & editing. YS: Data curation, Writing – review & editing. FX: Investigation, Project administration, Supervision, Writing – review & editing.

## **Funding**

The author(s) declare financial support was received for the research and/or publication of this article. This work was funded by the Special Program on Science and Technology Innovation Capacity Building of BAAFS (KJCX20230414) and the R&D Foundation of the Institute of Animal Husbandry and Veterinary Medicine, BAAFS (XMS202407).

### Conflict of interest

The authors declare that the research was conducted in the absence of any commercial or financial relationships that could be construed as a potential conflict of interest.

### Generative AI statement

The author(s) declare that no Generative AI was used in the creation of this manuscript.

# References

Baez, A., Sharma, A. K., Bryukhanov, A., Anderson, E. D., Rudack, L., Olivares-Hernandez, R., et al. (2022). Iron availability enhances the cellular energetics of aerobic *Escherichia coli* cultures while upregulating anaerobic respiratory chains. *New Biotechnol.* 71, 11–20. doi: 10.1016/j.nbt.2022.06.004

Baltes, N., Hennig-Pauka, I., and Gerlach, G. F. (2002). Both transferrin binding proteins are virulence factors in *Actinobacillus pleuropneumoniae* serotype 7 infection. *FEMS Microbiol. Lett.* 209, 283–287. doi: 10.1016/S0378-1097(02)00570-0

Beddek, A. J., Sheehan, B. J., Bossé, J. T., Rycroft, A. N., Kroll, J. S., and Langford, P. R. (2004). Two TonB systems in *Actinobacillus pleuropneumoniae*: their roles in iron acquisition and virulence. *Infection Immun.* 72, 701–708. doi: 10.1128/Iai.72.2.701-708.2004

Buettner, F. F. R., Bendalla, I. M., Bossé, J. T., Meens, J., Nash, J. H. E., Härtig, E., et al. (2009). Analysis of the *Actinobacillus pleuropneumoniae* HlyX (FNR) regulon and identification of iron-regulated protein B as an essential virulence factor. *Proteomics* 9, 2383–2398. doi: 10.1002/pmic.200800439

Buettner, F. F. R., Konze, S. A., Maas, A., and Gerlach, G. F. (2011). Proteomic and immunoproteomic characterization of a DIVA subunit vaccine against *Actinobacillus pleuropneumoniae*. *Proteome Sci* 9, 23. doi: 10.1186/1477-5956-9-23

Cassat, J. E., and Skaar, E. P. (2013). Iron in infection and immunity. *Cell Host Microbe* 13, 510-520. doi: 10.1016/j.chom.2013.04.010

Chung, J. W., Küster-Schöck, E., Gibbs, B. F., Jacques, M., and Coulton, J. W. (2012). Immunoproteomic analyses of outer membrane antigens of *Actinobacillus pleuropneumoniae* grown under iron-restricted conditions. *Veterinary Microbiol.* 159, 187–194. doi: 10.1016/j.vetmic.2012.03.038

de Almeida, M. N., Pineyro, P. P., Holtkamp, D., MaChado, I., Silva, A. P. S., Cezar, G., et al. (2025). Post-outbreak dynamics and persistence of *Actinobacillus pleuropneumoniae* serotype 15 in finisher pigs in Iowa. *Veterinary Res.* 56. doi: 10.1186/s13567-025-01538-4

del Río, M. L., Gutiérrez-Martín, C. B., Rodríguez-Barbosa, J. I., Navas, J., and Rodríguez-Ferri, E. F. (2005). Identification and characterization of the TonB region

Any alternative text (alt text) provided alongside figures in this article has been generated by Frontiers with the support of artificial intelligence and reasonable efforts have been made to ensure accuracy, including review by the authors wherever possible. If you identify any issues, please contact us.

### Publisher's note

All claims expressed in this article are solely those of the authors and do not necessarily represent those of their affiliated organizations, or those of the publisher, the editors and the reviewers. Any product that may be evaluated in this article, or claim that may be made by its manufacturer, is not guaranteed or endorsed by the publisher.

## Supplementary material

The Supplementary Material for this article can be found online at: https://www.frontiersin.org/articles/10.3389/fcimb.2025. 1669654/full#supplementary-material

#### SUPPLEMENTARY FIGURE 1

Growth curves of APP under different culture conditions. (A) Growth curves of APP in the TSB medium with addition of different concentrations of DFO. (B) Growth curves of APP in the TSB medium with or without addition of FeCl $_3$ .

#### SUPPLEMENTARY FIGURE 2

Metabolism pathway analysis between proteins in the cluster of shared DEGs/DEPs with the cluster of DEPs. The red line represented the pathways in the cluster of shared DEGs/DEPs, the green line represented the pathways affected by the cluster of DEPs. The metabolism pathway analysis was performed by iPath3.0 (https://pathways.embl.de/).

and its role in transferrin-mediated iron acquisition in. FEMS Immunol. Med. Microbiol. 45, 75–86. doi: 10.1016/j.femsim.2005.02.008

Deslandes, V., Nash, J. H. E., Harel, J., Coulton, J. W., and Jacques, M. (2007). Transcriptional profiling of *Actinobacillus pleuropneumoniae* under iron-restricted conditions. *BMC Genomics* 8, doi: 10.1186/1471-2164-8-72

Diarra, M. S., Dolence, J. A., Dolence, E. K., Darwish, I., Miller, M. J., Malouin, F., et al. (1996). Growth of *Actinobacillus pleuropneumoniae* is promoted by exogenous hydroxamate and catechol siderophores. *Appl. Environ. Microbiol.* 62, 853–859. doi: 10.1128/aem.62.3.853-859.1996

Dorman, D. C. (2023). The role of oxidative stress in manganese neurotoxicity: a literature review focused on contributions made by professor Michael Aschner. *Biomolecules* 13, doi: 10.3390/biom13081176

Ellermann, M., and Arthur, J. C. (2017). Siderophore-mediated iron acquisition and modulation of host-bacterial interactions. *Free Radical Biol. Med.* 105, 68–78. doi: 10.1016/j.freeradbiomed.2016.10.489

Frost, J. N., and Drakesmith, H. (2025). Iron and the immune system. *Nat. Rev. Immunol.* doi: 10.1038/s41577-025-01193-y

Goethe, R., Gonzáles, O. F., Lindner, T., and Gerlach, G.-F. (2000). A novel strategy for protective *Actinobacillus pleuropneumoniae* subunit vaccines: detergent extraction of cultures induced by iron restriction. *Vaccine* 19, 966–975. doi: 10.1016/s0264-410x(00)00212-7

Grosse, C., Scherer, J., Koch, D., Otto, M., Taudte, N., and Grass, G. (2006). A new ferrous iron-uptake transporter, EfeU (YcdN), from *Escherichia coli. Mol. Microbiol.* 62, 120–131. doi: 10.1111/j.1365-2958.2006.05326.x

Han, C., Shi, C. P., Liu, L. M., Han, J. C., Yang, Q. Q., Wang, Y., et al. (2024). Majorbio Cloud 2024: update single-cell and multiomics workflows. *iMeta* 3. doi: 10.1002/imt2.217

Hsu, Y. M., Chin, N., Chang, C. F., and Chang, Y. F. (2003). Cloning and characterization of the *Actinobacillus pleuropneumoniae fur* gene and its role in

regulation of ApxI and AfuABC expression. DNA Sequencing 14, 169-181. doi: 10.1080/1042517031000089469

Jacobsen, I., Gerstenberger, J., Gruber, A. D., Bossé, J. T., Langford, P. R., Hennig-Pauka, I., et al. (2005). Deletion of the ferric uptake regulator Fur impairs the *in vitro* growth and virulence of *Actinobacillus pleuropneumoniae*. *Infection Immun*. 73, 3740–3744. doi: 10.1128/lai.73.6.3740-3744.2005

Jacques, M. (2004). Surface polysaccharides and iron-uptake systems of Actinobacillus pleuropneumoniae. Can. J. Veterinary Research-Revue Can. Recherche Veterinaire 68, 81–85.

Kiel, M. C., and Ganoza, M. C. (2001). Functional interactions of an *Escherichia coli* ribosomal ATPase. *Eur. J. Biochem.* 268, 278–286. doi: 10.1046/j.1432-1033.2001.01873.x

Klitgaard, K., Friis, C., Angen, O., and Boye, M. (2010). Comparative profiling of the transcriptional response to iron restriction in six serotypes of *Actinobacillus pleuropneumoniae* with different virulence potential. *BMC Genomics* 11. doi: 10.1186/1471-2164-11-698

Kramer, J., Özkaya, Ö., and Kümmerli, R. (2020). Bacterial siderophores in community and host interactions. *Nat. Rev. Microbiol.* 18, 152–163. doi: 10.1038/s41579-019-0284-4

Li, M. N., Han, Q., Wang, N., Wang, T., You, X. M., Zhang, S., et al. (2024). 16S rRNA gene sequencing for bacterial identification and infectious disease diagnosis. *Biochem. Biophys. Res. Commun.* 739. doi: 10.1016/j.bbrc.2024.150974

Lill, R., and Freibert, S. A. (2020). Mechanisms of mitochondrial iron-sulfur protein biogenesis. *Annu. Rev. Biochem.* 89, 471–499. doi: 10.1146/annurev-biochem-013118-111540

Livak, K. J., and Schmittgen, T. D. (2001). Analysis of relative gene expression data using real-time quantitative PCR and the  $2^{-\Delta\Delta CT}$  method. *Methods* 25, 402–408. doi: 10.1006/meth.2001.1262

Loera-Muro, A., and Angulo, C. (2018). New trends in innovative vaccine development against *Actinobacillus pleuropneumoniae*. *Veterinary Microbiol.* 217, 66–75. doi: 10.1016/j.vetmic.2018.02.028

Mikael, L. G., Srikumar, R., Coulton, J. W., and Jacques, M. (2003). *fhuA* of *Actinobacillus pleuropneumoniae* encodes a ferrichrome receptor but is not regulated by iron. *Infection Immun.* 71, 2911–2915. doi: 10.1128/iai.71.5.2911-2915.2003

Miller, C. E., Williams, P. H., and Ketley, J. M. (2009). Pumping iron: mechanisms for iron uptake by *Campylobacter*. *Microbiology* 155, 3157–3165. doi: 10.1099/mic.0.032425-0

Moreno-Gámez, S. (2022). How bacteria navigate varying environments. Science 378, 845-845. doi: 10.1126/science.adf

Nielsen, K. K., and Boye, M. (2005). Real-time quantitative reverse transcription-PCR analysis of expression stability of *Actinobacillus pleuropneumoniae* housekeeping genes during *in vitro* growth under iron-depleted conditions. *Appl. Environ. Microbiol.* 71, 2949–2954. doi: 10.1128/Aem.71.6.2949-2954.2005

Peng, W., Yang, X., Yan, K., Chen, H. C., Yuan, F. Y., and Bei, W. C. (2021). CopA protects *Actinobacillus pleuropneumoniae* against copper toxicity. *Veterinary Microbiol.* 258. doi: 10.1016/j.vetmic.2021.109122

Qu, M. X., Li, L. L., Zan, X. Y., Cui, F. J., Sun, L., and Sun, W. J. (2025). Molecular characterization of a transcriptional regulator GntR for gluconate metabolism in industrial 2-ketogluconate producer JUIM01. *Microorganisms* 13. doi: 10.3390/microorganisms13061395

Rios-Delgado, G., McReynolds, Aubrey, K. G., Pagella, Emma, A., Norambuena, J., et al. (2025). The *Staphylococcus aureus* non-coding RNA IsrR regulates TCA cycle activity and virulence. *Nucleic Acids Res.* 53. doi: 10.1093/nar/gkae1243

Sassu, E. L., Bossé, J. T., Tobias, T. J., Gottschalk, M., Langford, P. R., and Hennig-Pauka, I. (2018). Update on *Actinobacillus pleuropneumoniae*-knowledge, gaps and challenges. *Transboundary Emerging Dis.* 65, 72–90. doi: 10.1111/tbed.12739

Sharma, S., Kaushik, V., Kulshrestha, M., and Tiwari, V. (2023). Different efflux pump systems in *Acinetobacter baumannii* and their role in multidrug resistance. *Adv. Exp. Med. Biol.* 1370, 155–168. doi: 10.1007/5584\_2023\_771

Soto Perezchica, M. M., Guerrero Barrera, A. L., Avelar Gonzalez, F. J., Quezada Tristan, T., and Macias Marin, O. (2023). *Actinobacillus pleuropneumoniae*, surface proteins and virulence: a review. *Front. Veterinary Sci* 10. doi: 10.3389/fvets.2023.1276712

Spiga, L., Fansler, R. T., Perera, Y. R., Shealy, N. G., Munneke, M. J., David, H. E., et al. (2023). Iron acquisition by a commensal bacterium modifies host nutritional immunity during *Salmonella* infection. *Cell Host Microbe* 31, 1639–1654. doi: 10.1016/j.chom.2023.08.018

Srikumar, R., Mikael, L. G., Pawelek, P. D., Khamessan, A., Gibbs, B. F., Jacques, M., et al. (2004). Molecular cloning of haemoglobin-binding protein HgbA in the outer membrane of *Actinobacillus pleuropneumoniae*. *Microbiology* 150, 1723–1734. doi: 10.1099/mic.0.27046-0

Stoffel, N. U., and Drakesmith, H. (2024). Effects of iron status on adaptive immunity and vaccine efficacy: a review. Adv. Nutr. 15, 100238. doi: 10.1016/j.advnut.2024.100238

Stringer, O. W., Bossé, J. T., Lacouture, S., Gottschalk, M., Fodor, L., Angen, O., et al. (2021). Proposal of *Actinobacillus pleuropneumoniae* serovar 19, and reformulation of previous multiplex PCRs for capsule-specific typing of all known serovars. *Veterinary Microbiol.* 255. doi: 10.1016/j.vetmic.2021.109021

Subhadra, B., Surendran, S., Lim, B. R., Yhn, J. S., Kim, D. H., Woo, K., et al. (2020). Regulation of the AcrAB efflux system by the quorum-sensing regulator AnoR in *Acinetobacter nosocomialis. J. Microbiol.* 58, 507–518. doi: 10.1007/s12275-020-0185-2

Tang, H., Zhang, Q. H., Han, W. Y., Wang, Z. Y., Pang, S. Q., Zhu, H., et al. (2022). Identification of FtpA, a Dps-like protein involved in anti-oxidative stress and virulence in *Actinobacillus pleuropneumoniae*. *J. Bacteriology* 204. doi: 10.1128/jb.00326-21

Whitby, P. W., Seale, T. W., Morton, D. J., VanWagoner, T. M., and Stull, T. L. (2010). Characterization of the *Haemophilus* influenzae *tehB* gene and its role in virulence. *Microbiology* 156, 1188–1200. doi: 10.1099/mic.0.036400-0

Xie, F., Wang, Y. L., Li, G., Liu, S. H., Cui, N., Liu, S. G., et al. (2017). The SapA protein is involved in resistance to antimicrobial peptide PR-39 and virulence of *Actinobacillus pleuropneumoniae*. Front. Microbiol. 8. doi: 10.3389/fmicb.2017.00811

Zhang, L. J., Luo, W. T., Xiong, R. Y., Li, H. T., Yao, Z. M., Zhuo, W. X., et al. (2022). A combinatorial vaccine containing inactivated bacterin and subunits provides protection against *Actinobacillus pleuropneumoniae* infection in mice and pigs. *Front. Veterinary Sci* 9. doi: 10.3389/fvets.2022.902497